www.czasopisma.pan.pl PAN www.journals.pan.pl
POLSKA AKADEMIA NAUK

Arch. Min. Sci. **65** (2020), 4, 901-916
Electronic version (in color) of this paper is available: http://mining.archives.pl

DOI 10.24425/ams.2020.135184

PRZEMYSŁAW SKOTNICZNY[1*]

AEROLOGICAL FACTORS FAVOURING THE OCCURRENCE OF ENDOGENOUS FIRES ON COAL WASTE STOCKPILES

Coal waste stockpiles – as artificial formations being a result of the exploitation of underground coal deposits – are constantly influenced by external factors, such as rock mass movements affecting the stability of the stockpile body and changing weather conditions, leading to a cycle of aerological phenomena which intensify the self-heating of the deposited material. Together with the occurrence of external factors, the stored material is also characterised by a set of internal features (also called genetic) that have a direct impact on the kinetics of the self-heating reaction.

The paper focuses mainly on the issue of external factors such as the inclination angle of the stockpile, erosion of the slopes and thermal insulation of the layers of the stored material, which affect the phenomenon of self-heating of the material. Studies of impact of these factors on the thermal stability of coal waste stockpiles are important in the aspect of secondary exploitation of the stockpiles as well as during their reclamation or revitalisation. The numerical solutions presented in the paper should be treated as guidelines that define the directions of analysis for specific cases.

Keywords: coal waste stockpile, endogenous fires, stockpile reclamation, numerical analysis

1. Introduction

At present, there are over 200 coal waste stockpiles in the mining areas covering the area of Upper and Lower Silesia [1]. In the vast majority of cases those stockpiles – due to the composition of the deposited material – are characterised as suitable for repeated mining operations [2]. However, the authors dealing with the issues of stockpile reclamation/revitalisation [2-5] pay attention to the problem of potential endogenous fire outbreaks as a result of stockpile structure breaching.

[1] STRATA MECHANICS RESEARCH INSTITUTE POLISH ACADEMY OF SCIENCES, 27 REYMONTA STR., 30-059 KRAKOW, POLAND

* Corresponding author: przemyslaw.skotniczny@imgpan.pl

The phenomenon of endogenous fire in coal waste stockpiles is a long-term process. According to many years of experimentation [5-7], the development from the safe state to the occurrence of all fire symptoms lasts from 12 to 16 months.

The basic problem that emerges during the analysis of the risk of endogenous fires is the proper identification of factors that may have a significant impact on the intensity of the phenomena. The factors that influence the intensity of reactions which may lead to an endogenous fire can generally be divided into two groups, i.e. internal factors (sometimes called genetic factors) and external factors.

The first group includes:

- chemical composition of the deposited material, including moisture content,
- petrographic composition.

The external factors can include:

- shape of the slopes of the stockpile,
- bulk density of the material, which affects the porosity and permeability of the individual layers of the deposited material,
- stockpile slope erosion,
- distribution of average annual wind speeds (rose of the winds) and barometric pressure changes in the stockpile surroundings,
- the difference in the values of heat conduction coefficients of individual layers of the stockpile, created during the formation or reclamation of the stockpile.

The genetic factors that have an influence on the phenomenon of endogenous fires in coal waste stockpiles are an immanent feature of the deposited material. Any attempt to affect and improve the properties of the waste in terms of reducing its tendency to self-heat involves additional treatment, which may be technically difficult and economically unjustified. Therefore, it seems appropriate to focus on reducing the negative impact of external factors on the intensity of processes originating from physical and chemical reactions.

On the other hand, the features listed in the group of internal factors mainly affect the intensity of the phenomenon of self-heating of the deposited material. There are a number of theories that bring this phenomenon closer [14]. However, regardless of which theory is considered to be the leading one, physical and chemical parameters of coal, the remains of which – either post-flotation waste or excavated material – form individual layers of the stockpile, have a significant impact on the temperature increase inside the stockpile.

Authors of works devoted to the phenomenon of coal self-heating [3, 4] draw attention to one important feature of the process. In any case, oxygen contained in the ambient air is needed to initiate the process. This observation directly leads us to focus on the mechanisms of gas exchange between the body of the stockpile and the environment.

Among various external factors that may affect the occurrence of endogenous fires, three should be distinguished, which – based on many years of research [15,16] – show the highest significance. They include among others:

- shape of the slopes of the stockpile,
- stockpile slope erosion,
- degree of thermal insulation between individual layers of the deposited material.

The above factors are of particular importance when they are additionally correlated with the average annual distribution of wind directions around the stockpile (so-called rose of the winds).

2. Model research studies

A numerical analysis is the most effective technique for analysing the impact of flow parameter variability in complex geometries [3,4,8-11]. Numerical solutions work particularly well in a multivariate analysis and significantly reduce the time between noticing a problem and making a decision.

The results of numerical simulations of the impact of the discussed factors on the intensity of stockpile volume aeration are presented below, which translates directly into an increase in the tendency of the deposited material to cause an endogenous fire.

Due to the fact that the flow conditions place the cases discussed in this paper in the area of turbulent flows for which there are no general solutions of the equations of motion due to the presence of an additional member expressing turbulent stresses [13]. The missing closing member in the equations describing the effects associated with turbulent motion was taken into account using the ***k-ω-SST*** model [12].

Closure of equations of motion is expressed by the following equations that describe, respectively, the transport of turbulence kinetic energy k (1) and the dissipation rate ω (2) [12]:

$$\frac{\partial}{\partial t}(\rho k)+\frac{\partial}{\partial x_i}(\rho k u_i)=\frac{\partial}{\partial x_j}\left(\Gamma_k\frac{\partial k}{\partial x_j}\right)+\tilde{G}_k-Y_k+S_k \tag{1}$$

$$\frac{\partial}{\partial t}(\rho \omega)+\frac{\partial}{\partial x_i}(\rho \omega u_i)=\frac{\partial}{\partial x_j}\left(\Gamma_\omega\frac{\partial \omega}{\partial x_j}\right)+G_\omega-Y_\omega+S_\omega+D_\omega \tag{2}$$

where $\tilde{G}_k$ means the production of turbulence kinetic energy as a function of average speed gradient, expressed by the following equation:

$$\tilde{G}_k=\min(G_k,10\rho\beta^* k\omega) \tag{3}$$

G_ω is the member used to describe production w expressed as:

$$\tilde{G}_\omega=\frac{\alpha}{\nu_t}G_k \tag{4}$$

where α is a coefficient expressed as the following relationship:

$$\alpha=\frac{\alpha_\infty}{\alpha^*}\left(\frac{\alpha_0+\mathrm{Re}_t/R_\omega}{1+\mathrm{Re}_t/R_\omega}\right) \tag{5}$$

defined with appropriate fixed models.

The expressions appearing in equations (1) and (2), i.e.

Γ_k and Γ_ω mean, respectively, effective diffusivity k and ω, as determined by the following dependencies:

$$\Gamma_k=\mu+\frac{\mu_t}{\sigma_k} \tag{6}$$

$$\Gamma_\omega = \mu + \frac{\mu_t}{\sigma_\omega} \tag{7}$$

in which σ_k and σ_ω determine the turbulent Prandtl number for k and ω.

Y_k and Y_ω mean dissipation k and ω,

$$Y_k = \rho\beta^* k_\omega \tag{8}$$

$$Y_\omega = \rho\beta^* \omega^2 \tag{9}$$

and, in turn, member D_ω means cross-diffusion, defined as:

$$D_\omega = 2(1-F_1)\rho\sigma_{\omega,2}\frac{1}{\omega}\frac{\partial k}{\partial x_j}\frac{\partial \omega}{\partial x_j} \tag{10}$$

Additionally, due to the need to determine the values characterising the flow of values also inside the stockpile body, it was necessary to activate the appropriate source member in the equations of motion. The general form of the formula is described in equation 11.

$$S_i = -\left(\sum_{j=1}^{3} D_{ij}\mu v_j + \sum_{j=1}^{3} C_{ij}\frac{1}{2}\rho v_j^2\right) \tag{11}$$

When considering the flow in a homogeneous medium, the above equation may take the following form:

$$S_i = -\left(\frac{\mu}{\alpha}v_i + C_2\frac{1}{2}\rho v_i^2\right) \tag{12}$$

All numerical simulations presented in the paper were made in the software package CFD – Ansys FLUENT.

2.1. Shape of stockpile slopes (inclination angle)

The basic geometrical feature of a stockpile is the shape of its surface, especially the inclination angle of slopes. Nowadays, the newly built stockpiles have a prism structure. This is due to the way waste is deposited; the stockpiles created in the early stages of mining were placed near mining shafts, using handling equipment (trolleys, cable car), which resulted in stockpiles of conical shape. With an increasing distance between mining shafts and stockpiles, the concept of using handling equipment was abandoned in favour of more economical wheeled transport.

Geometry of the discussed cases

For the purpose of analysing the influence of the inclination angle of stockpile slopes, five geometrical models in the shape of a truncated pyramid (which simulates a prism-shaped stockpile, Fig. 1) were created. The common feature of all the models was the surface area of the base of the pyramid. Five inclination angles of the slope to the base were considered, i.e. $\alpha = 69°, 67°, 63°, 60°$ and $35°$. The corresponding dimensionless total volumes of the stockpiles

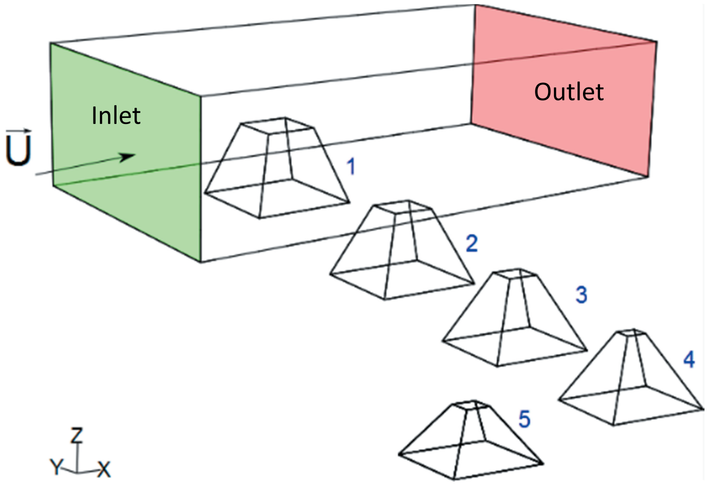

Fig. 1. The series of types of analysed models of prism-shaped stockpiles

were respectively: $V_1 = 1$, $V_2 = 0.9$, $V_3 = 0.8$, $V_4 = 7$, and $V_5 = 0.56$, where volume is defined as V/V_1, and V_1 is the volume of the first model.

After numerical determination of the flow around these five geometrical cases for the value of air inflow velocity totalling $U = 5$ m/s, the influence of the inclination angle of the slope to the base of the pyramids on the distribution and value of static pressure from the windward side was estimated. The results are presented in Fig. 3.

2.2. Computational grid, boundary conditions

Geometries (Fig. 1), creating calculation domains discretised with *quad-pave* unstructured mesh, were designed to perform the calculations. A fragment of the mesh covering the slopes of the model No. 1 is presented in Fig. 2. Due to the computation time and the fact that the results

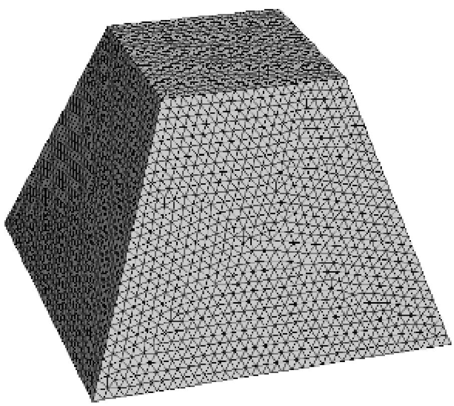

Fig. 2. Model of the stockpile discretised with tri-pave mesh

are used for qualitative analysis, it was decided to use the default mesh proposed by the pre-processor algorithms. The total number of elements in the computational meshes ranged from about 500,000 to 700,000 depending on the model analysed (model 1 had the most rough mesh).

The calculations were performed in the ANSYS Fuent solver, for the turbulent flow case, using the *k-ω-SST*, stationary and isothermal model. The air stream velocity in the inlet section to the computational domain was $U = 5$ m/s. All models of stockpiles were treated as porous media with the assumed parameters [17]:

– Porosity $\varepsilon = 0.3$,
– Permeability coefficient $\alpha = 10^{-9}$ m^2.

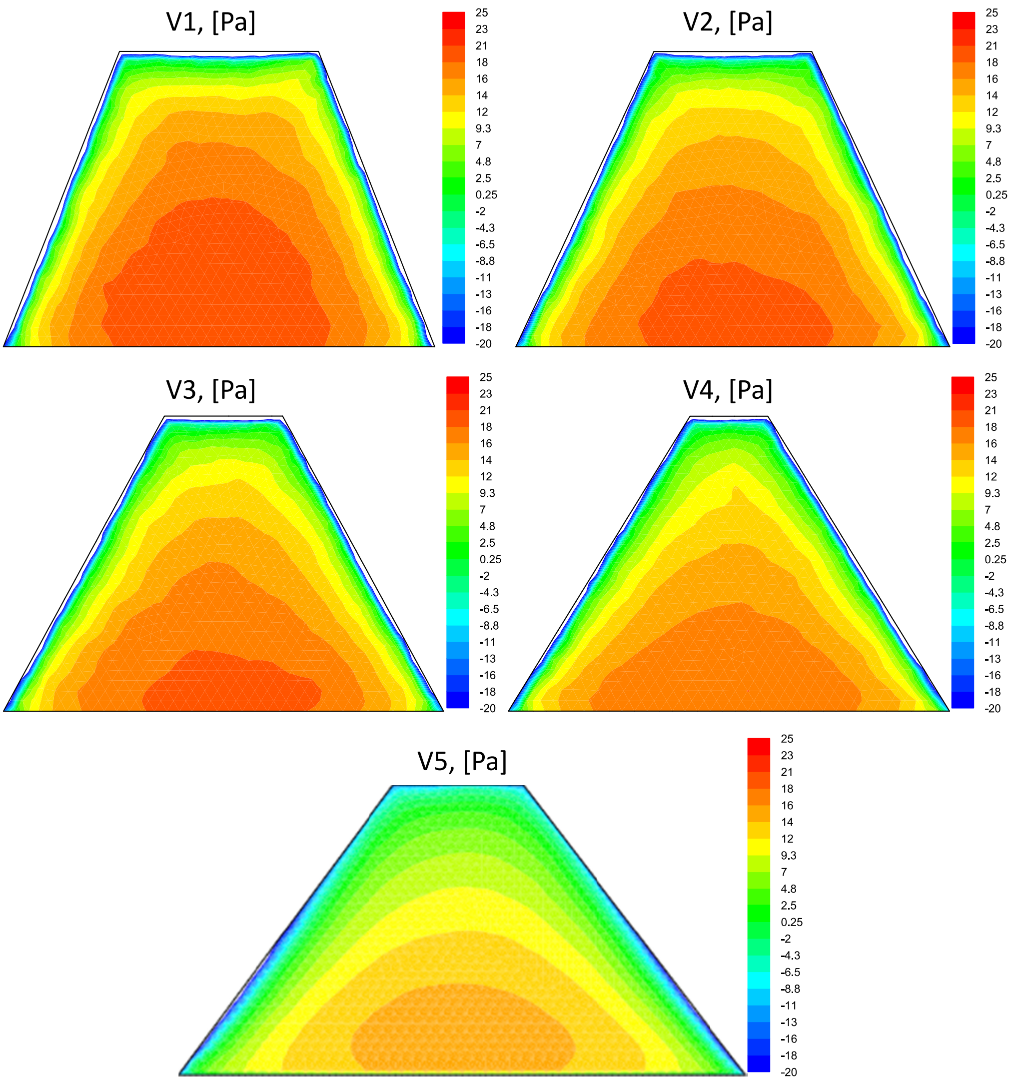

Fig. 3. Static pressure distributions on the slopes of a prism-shaped stockpile. Explanation in the text

Fig. 3 shows the projections of slopes of a prism-shaped stockpile on a plane perpendicular to the flow with colourful static pressure distributions. When analysing the cases (*V*1 to *V*5), it is possible to notice a decrease in the area of occurrence of the maximum total pressure together with a decrease in the slope inclination angle to the base of the stockpile. As the angle of inclination is reduced, the maximum value of the calculated static pressure (figures are made using the same colour scale from –20 to 25 Pa) also decreases; for *V*1 geometry – *Ps* max = 25 Pa, for *V*5 geometry – *Ps* max = 13 Pa. This phenomenon can be seen more clearly in Fig. 4, which shows the change in the static pressure value on the central line of the slope from the windward direction as a function of the height of the stockpile.

On the other hand, the distinctive zones of high negative pressure – totalling approximately p_s = –20 Pa – visible on the edges of the slopes, are due to the nature of air flow in the surrounding of the porous solid.

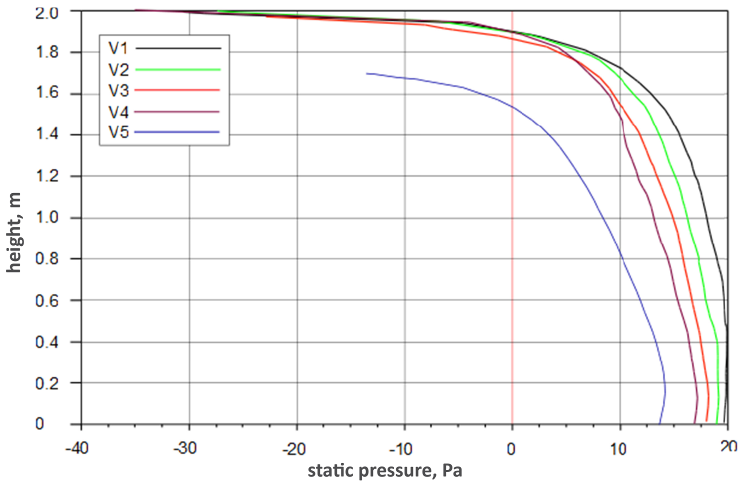

Fig. 4. Static pressure distribution on the windward side of the slope

The area of maximum static pressure on the slope for the *V*1 geometry (black line in Fig. 4) is much wider and reaches 0.4 m of the solid's height as compared to other cases. The smallest static pressure values on the central line of the slope are observed for the *V*5 geometry. However, in this case, the total volume of the deposited material is up to 40% less than in other cases. The issue of total pressure distribution on the slopes of the stockpile was discussed based on simple geometry, but in reality, with much more complicated shapes of the stockpile body, similar results can be expected.

2.3. Stockpile slope erosion

In order to model the effect of stockpile slope erosion on the increase in the risk of endogenous fires, appropriate geometry had to be created. The *V*1 geometry discussed in the previous subsection (Fig. 1) was taken as the starting point. The modification involved extending the flow issue with an additional factor, i.e. porosity of the stockpile material.

The view of the geometry analysed in this chapter is shown in Fig. 5. The visible crevice was designed as a separate geometrical solid, being a common part of the geometrical model. Both the stockpile body and the crevice were designed as porous materials that differed in the value of porosity ε and permeability k parameters (Table 1).

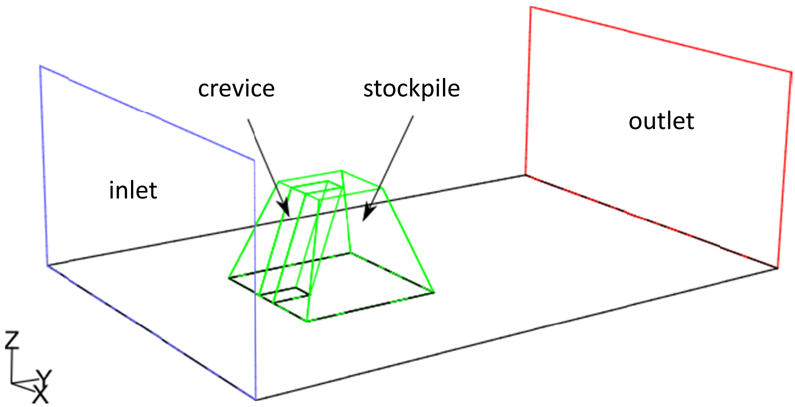

Fig. 5. Geometrical model of the stockpile with an erosion crevice on the slope from the windward side

TABLE 1

Values that characterise porous material

Name	ε	k	**C2**
Stockpile	0.3	1e-6	100
Crevice	0.9	1e-1	1

Since the numerical experiment in question was of a demonstrative nature, the values of the porosity, permeability and C2 parameters were adopted in the order of magnitude, consistent with the actually measured values of the stockpile material [17].

The results of the experiment are presented in a graphical form in Fig. 6 and Fig. 7.

In order to facilitate the comparison, the values of pressure distributions (Fig. 6) are presented as normalised values $p_n = p/p_{\max}$. On the other hand, the speed inside and outside the stockpile model (Fig. 7) is presented as filtered distributions in the range 0-0.5 m/s.

Owing to the distribution of pressures on the slope from the leeward direction, the assumed permeability of the material enables penetration of the top layers of the stockpile (Fig. 6A). In the area where high differences in pressure occur, i.e. in the summit zone, the penetration of deep layers is particularly intense (Fig. 6A).

The occurrence of loosened and thus more porous material in the volume imitating an erosion crevice in the slope of the excavation causes increased propagation of the mass of flowing air in the stockpile volume. The distribution of static pressures on the slope, shown in Fig. 6B, has a much greater range than in the case described in Fig. 6A. This phenomenon has a direct impact on increasing the value of the velocity vector inside the stockpile (Fig. 7B). As a result, the stockpile with erosion crevices on the slopes is better aerated and, consequently, the risk of endogenous fire increases.

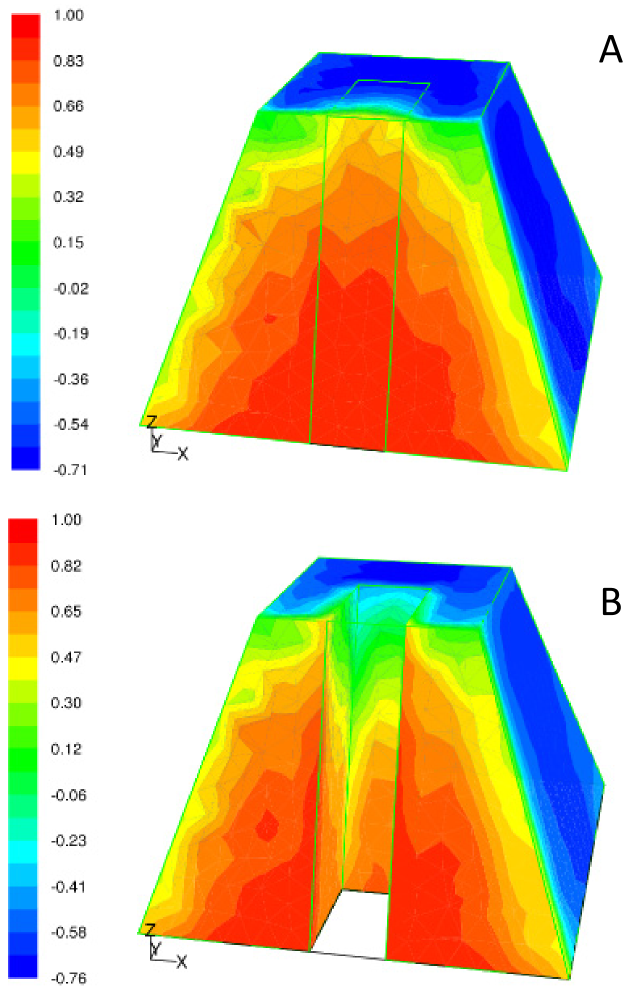

Fig. 6. Distribution of normalised pressure values p_n on the slope of the stockpile model.
A) case without a crevice, B) case with a crevice

The photograph below (Fig. 8) shows an erosion crevice created at the top of a coal waste stockpile.

The occurrence of stockpile discontinuity in this place intensified the thermal processes taking place inside the stockpile. The photograph (Fig. 8) clearly shows smoke coming out of the crevice.

2.4. Impact of insulating layers

Additional sealing layers, which are formed alternately with the proper material, are used quite often when depositing coal waste. This procedure is widely applied especially during reclamation of thermally active stockpiles. Its purpose is to additionally seal the individual layers

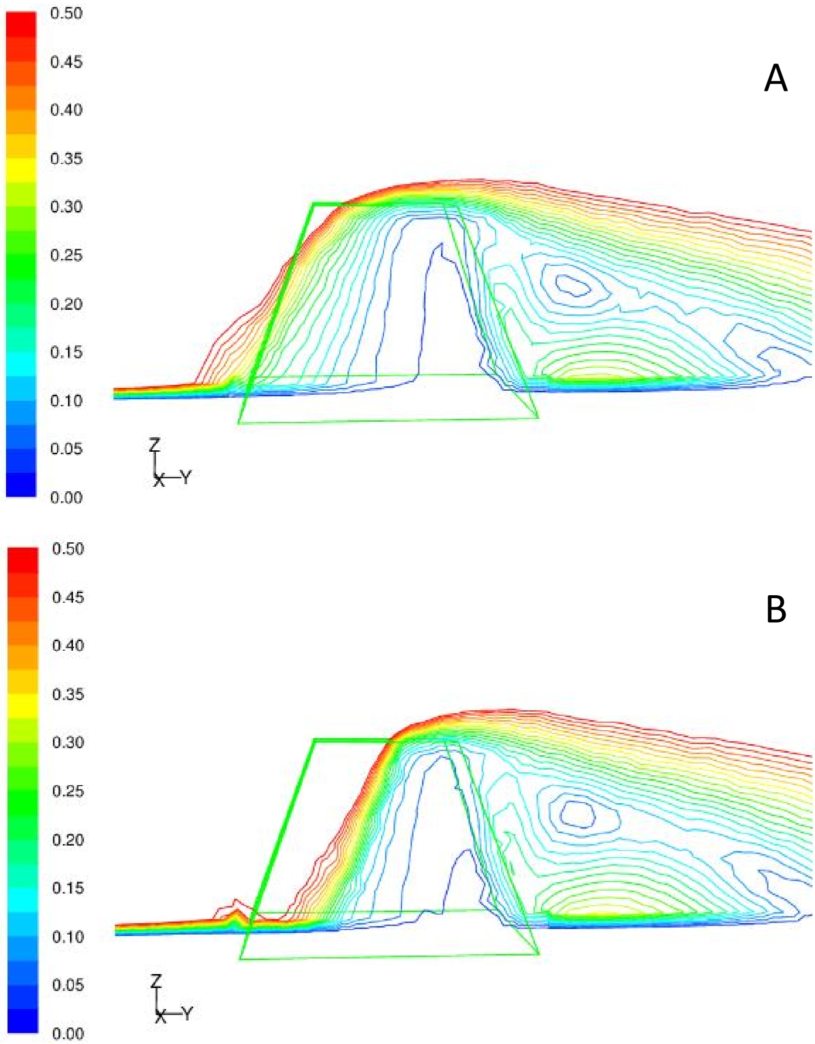

Fig. 7. Filtered distribution of speed inside and outside the stockpile model in a plane parallel to the flow direction of U_∞ speed on the model axis. A) without a crevice, B) with a crevice

of the deposited material. When applied precisely and consistently, the sealing system has the advantage of reducing the aeration of the stockpile solid. However, there is a risk that during the reclamation of a stockpile whose material was sufficiently cooled down the sealing process may increase the risk of recurrence of an endogenous fire.

We should consider the following example.

The coal waste stockpile was subject to reclamation by means of sealing with layers. The longitudinal section of the fragment of the stockpile is shown in Fig. 9. The layers, consisting of three cells each, marked in Fig. 9 with symbols from a1 to a28, form an alternate structure.

Fig. 8. Erosion crevice on a coal waste stockpile

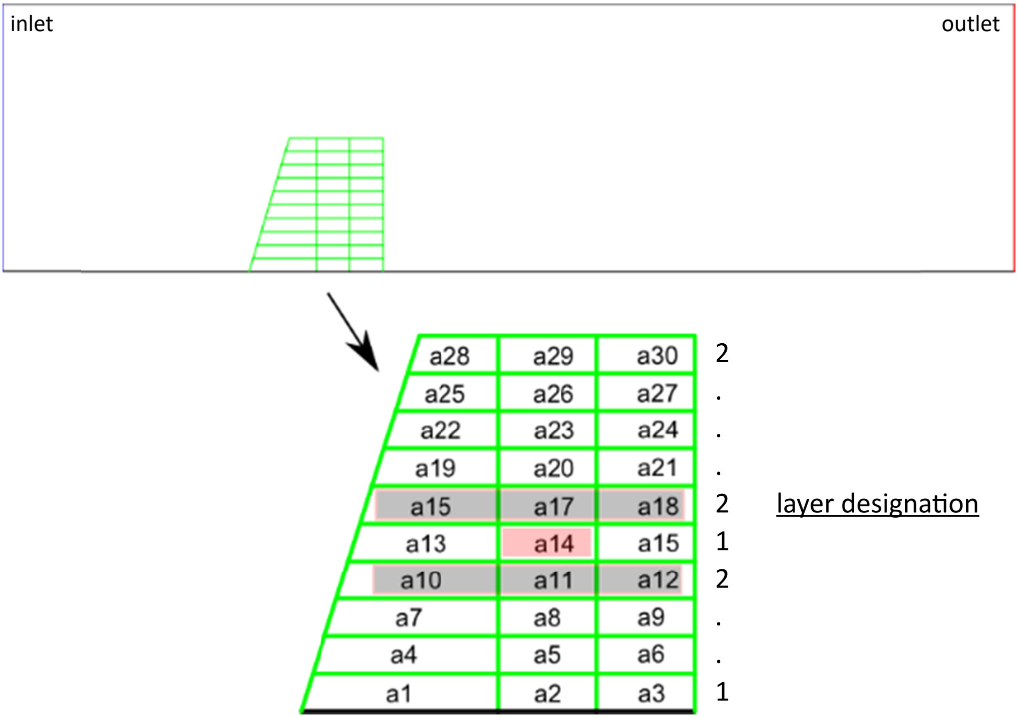

Fig. 9. Longitudinal section through a sealed coal waste stockpile

The distribution of the cells in the layers results from the applied stratification and thickening technology. To simplify the model, it was assumed that the individual cells in a given layer would have the same parameters. Table 2 presents the numerical values of two layers which alternately form a stockpile.

TABLE 2

Layer parameters

Layer No	**Porosity** ε **[%]**	**Permeability** k **[m^2]**	**Conductivity coefficient** λ **[W/mK]**
1. deposited layer	0.3	$1e^{-6}$	0.5
2. sealing layer	0.3	$1e^{-6}$	0.173

The layer of deposited material marked as 1 consists of cells from $a1$ to $a3$; the sealing layer above it, marked as 2, consists of cells from $a4$ to $a6$. Subsequent layers occur alternately. In addition, a volumetric heat source with an output of 10 kW/m^3 was placed in the $a14$ cell. This source simulates the occurrence of a concentrated area of increased thermal activity, resulting from, e.g., bad cooling of masses during the process of stockpile reclamation.

The task formulated in this way was then designed and calculated in Ansys FLUENT. The results of the simulation are presented in Figure 10.

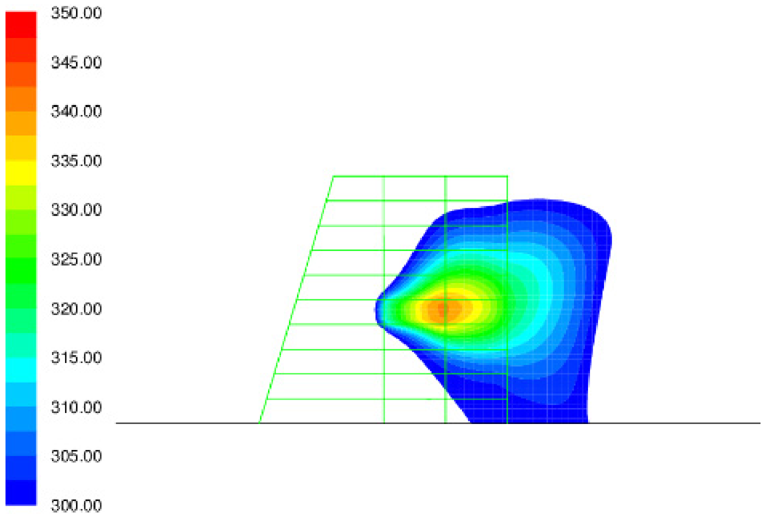

Fig. 10. Temperature distribution inside the stockpile for alternately positioned sealing layers. Temperature scale in K

The shape and distribution of isotherms (Fig. 10) suggests a correlation between the existence of sealing layers and the way the energy is transported inside the stockpile. The presence of layers that differ only in the conductivity coefficient (Table 2) results in strong anisotropic temperature distribution inside the stockpile.

For comparison, Fig. 11 presents the results of a numerical simulation of a case similar in terms of boundary values (air speed around the stockpile, material porosity, heat energy production in the source). The main difference between the case whose results are presented in Fig. 9 is the lack of alternately positioned insulation layers.

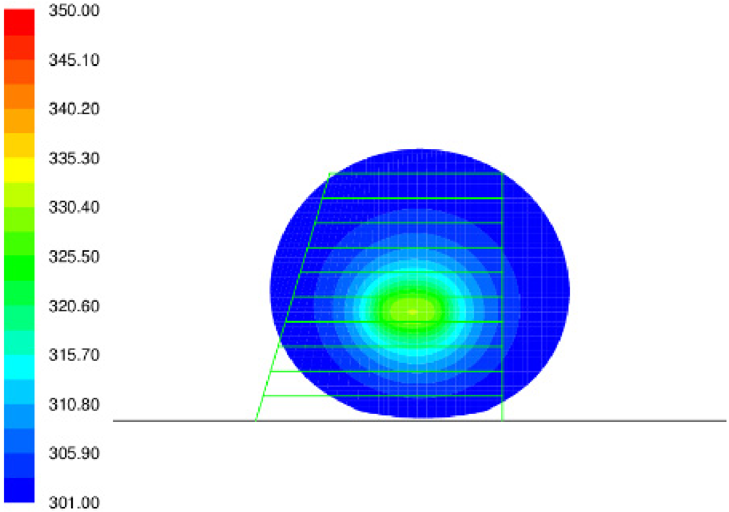

Fig. 11. Temperature distribution inside the stockpile in the case of lack of alternately positioned sealing layers. Temperature scale in K

It can be clearly seen that the lack of sealing layers in the latter case enables a more efficient energy exchange between the individual cells in the stockpile model, which directly affects a lower temperature value in the source.

This phenomenon is better illustrated by the graph in Fig. 12. The change of temperature in the source for the numerical simulation in time from $t_1 = 0$ s to $t_2 = 2000$ s shows big differences for both cases. The temperature for the stockpile with sealing layers has an upward tendency, which may cause the critical temperature value to be exceeded and the initiation of an endogenous fire process [14]. In turn, the lack of sealing layers causes greater energy dissipation, which helps to keep the source within safe temperatures (below the critical temperature).

3. Final remarks

It should be borne in mind that the case studies presented in this paper are for illustrative purposes. In fact, the impact of external factors on the phenomenon of endogenous fires inside a stockpile is of a combined nature. For example, it is not possible to talk only about the negative influence of the angle of inclination of stockpile slopes, regardless of the condition of their surface, the rose of the winds, the way the material is compacted, the presence of sealing layers, etc.

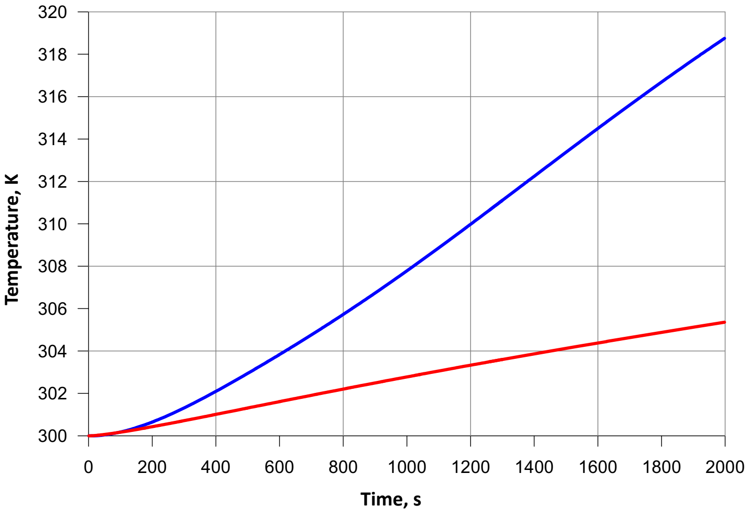

Fig. 12. Temperature increase over time in the source (a14)
blue – the case with sealing layers; red – the case without sealing layers

In spite of this preliminary remark, on the basis of the numerical analyses presented in the paper, some regularities can be found, which illustrate the scale of the problem and indicate possible corrections in the existing geometrical structure of a coal waste stockpile.

The planning and subsequent operation of a stockpile is a major logistical undertaking. For this reason, two main stages can be distinguished in view of the simulation material cited in the study:

Stockpile design

At this stage, the following are particularly important:

- meteorological data,
- the total planned volume of post-mining waste.

In terms of meteorological data, the most important is the rose of the winds estimated for the area of interest. The knowledge of average annual distributions of wind directions and values will enable the stockpile body to be rationally located and shaped as well as will minimise the risk of high pressure values on its slopes (Fig. 3). Due to local elevation data, it is important that the rose of the winds is defined as close to the area of interest as possible. Another meteorological factor that can facilitate the design process is the total amount of precipitation. This value affects the erosion of stockpile slopes (Fig. 6 and 7), especially in the initial phase of its operation, when the vegetation cover is still poorly developed. In addition, being aware of the risk of erosion caused by rainwater may also affect the design of the intermediate and target shape of the stockpile – for areas with an increased value of total precipitation, the number of technological routes, i.e. the number of so-called "shelves", should be greater. This will enable, above all, easy access to the places where current reclamation works will have to be carried out and will shorten the total length of a single slope, which is not insignificant in terms of washing out of material from the slope of the stockpile with flowing rainwater.

In turn, the knowledge of the planned sum of the volume of the deposited mass as a function of the total surface area for the stockpile will make it possible to design a stockpile with optimal slope angles. Obviously, it should be remembered that optimisation of the inclination angle affects the total volume of the stockpile body. In case of a mismatch between V_{max} and A_{max} (maximum volume to maximum surface area of the stockpile) a combined variant is possible, which involves creating a stockpile with different inclination angles of the slopes. However, this option requires additional data in the form of simulation analyses and a multi-year rose of the winds.

Stockpile operation

Two main directions of activities should be distinguished at the operation stage:

- precise documentation of the material deposited,
- continuous monitoring of sites at risk.

Data on current petrographic composition, origin (tailings, mining waste), moisture content, material temperature, etc. will facilitate a decision on how to deal with ongoing waste transport. For example, access material consisting mainly of gangue is less susceptible to self-heating than, for example, post-flotation sludge containing a certain amount of easily oxidising substances, and can be deposited in places more susceptible to aeration. Data obtained from the predicted computer simulation of individual stages of stockpile formation may be useful when making a decision at this point.

The need for year-round monitoring of selected stockpile sites is undeniable. Despite the existence of excellent tools for numerical analysis of mass and energy exchange phenomena, experimental data are considered the primary information. This is mainly due to the fact that a numerical model is not able to fully reflect the complexity of the flow and thermal (impact of the insulting layers combined with slope degradation) phenomena occurring in the stockpile – air complex. Remote monitoring seems useful as it eliminates the inconvenience of manual measurements over vast areas of the stockpile, allows a much larger number of measurements per day to be obtained and enables perfect repeatability as to the place of measurement.

References

[1] Marcisz M., Probierz K., Gawor Ł., *Possibilities of reclamation and using of large-surface coal mining dumping grounds in Poland*. Mineral Resources Management **36** (1), 105-122 (2020).

[2] Różański Z., *Recovery of the raw materials as an element of coal waste management and reusing of landfill sites*. Mineral Resources Management **35** (4), 147-162 (2019).

[3] Ejlali A., Aminossadati S.M., *Numerical analysis of fluid flow and heat transfer through a reactive coal stockpile*. Final report European Commission Directorate General XII Science, Research and Development Contract EV5V–CT94-0531, WS Atkins Consultants Ltd., Surrey, 1997.

[4] Siyakatshana N., Onno Ubbink, Kekana J., Wessels G., *Steady state cfd modelling of carbon dioxide release and Methananogenesis in coal heaps*. Second African Conference on Computational Mechanics – An International Conference – AfriCOMP11 January 5-8, 2011, Cape Town.

[5] Drenda J., Różański Z., Słota K., Wrona P., *Likwidacja zapożarowania elementem rekultywacji składowiska odpadów powęglowych w Siemianowicach Śląskich Bańgowie*. Zeszyty Naukowe Politechniki Śląskiej nr 272, p. 31-39, Gliwice 2006.

[6] Drenda J., Różański Z., Słota K., Wrona P., *Zagrożenie pożarowe na zwałowiskach odpadów powęglowych*. Górnictwo i Geoinżynieria **31**, 3/1, 149-157 (2007).

[7] Korski J., Henslok P., Bodynek P., *Doświadczenia z likwidacji zapożarowania składowiska odpadów powęglowych „Skalny" w Łaziskach Górnych*. ZN Politechnika Śląska seria Górnictwo, z. 261 (2004).

[8] Sensogut C., Ozdeniz A.H., *Statistical modelling of stockpile behaviour under different atmospheric conditions – Western Lignite Corporation (WLC) case*. Fuel **84**, 1858-1863 (2005).

[9] Hall R.C. (Ed.), *Evaluation of modeling uncertainty. CFD modeling of near-field atmospheric dispersion*. Project EMU (1997).

[10] Dziurzynski W., Krach A., Palka T., *Computer simulation of the propagation of heat in abandoned workings insulated with slurries and mineral substances*. Archives of Mining Sciences **59**, 1, 3-23 (2014).

[11] Krawczyk J., Janus J., *Modeling of the Propagation of Methane from the Longwall Goaf, Performed by Means of a Two-Dimensional Description*. Archives of Mining Sciences **59**, 4, 851-868 (2014).

[12] Fluent User Manual 2006 (wersja elektroniczna).

[13] Elsner J.W., *Turbulencja przepływów*. PWN, Warszawa 1985.

[14] Maciejasz Z., Kruk F., *Pożary podziemne w kopalniach*. Część 2, Wydawnictwo Śląsk, 1977.

[15] Korski J., Friede R., Henslok P., *Likwidacja egzogenicznych ognisk pożarowych składowiska odpadów pogórniczych „Waleska" w Łaziskach Górnych*. Zeszyty Naukowe. Górnictwo / Politechnika Śląska, z. 271, s. 83-96 (2006).

[16] Różański Z., *Management of mining waste and the areas of its storage – environmental aspects*. Mineral Resources Management **35** (3), 119-142 (2019).